

Figure 3 The expression of C68 rescued a defect in the assembly of PS1ΔC66 with APH-1 and NCT. (A) After APP695 and the indicated exogenous PS cofactors were retrovirally expressed with PS1ΔC66 and C68 or C68ΔC7 in PS-null cells. CHAPSO-solubilized lysate (1 mg) was immunoprecipitated (IP) with the anti-PS1 NTF antibody (H-70) and then immunoblotted with the anti-PS1 NTF antibody (Chemicon International, Inc.), anti-APH-1b antibody, anti-FLAG antibody, anti-NCT antibody and anti-PS1C-20 antibody. n-IgG, normal IgG (control for the anti-PS1NTF antibody). (B) The CHAPSO-solubilized lysate (1 mg) used in lanes 6 and 8 of A was immunoprecipitated (IP) with the anti-NCT antibody and then immunoblotted with the anti-NCT antibody, anti-PS1C-20 antibody (for the detection of C68 or C68ΔC7) and the anti-PS1 NTF antibody. n-IgG, normal IgG (control for the anti-NCT antibody). Data are representative of two independent experiments.

Thus, APH-1 is likely to stabilize the C37 fragment, although, at present, the exact reason for this is not known. We next determined whether TM8 is involved in the assembly of the active γ-secretase complex. As shown in Fig. 5, APH-1b and NCT were co-immunoprecipitated using the anti-PS1 NTF antibody when PS1ΔC37 and C37 were co-expressed, although the anti-PS1 antibody did not co-immunoprecipitate APH-1b and NCT when PS1ΔC66 and C37 were co-expressed. PEN-2 was also co-immunoprecipitated in both cases

(Fig. 5, lanes 2 and 4). Interestingly, C37 was also co-immunoprecipitated with PS1ΔC37, PS1 CTFΔC37, NCT, APH-1, and PEN-2, indicating that all truncated PS fragments, including CTFΔC37, constitute the active γ-secretase complex (Fig. 5). These results indicate that TM8 is involved in the PS1 complex assembly with NCT and APH-1b, and in PS endoproteolysis. Although C68 has the domain(s) for the binding of NCT and APH-1 (Supplementary Fig. S1), at present, we failed to determine by co-immunoprecipitation whether C37 has such domains, because C37 was unstable in the absence of PS1ΔC37 (data not shown). However, a previous study using a chimeric protein of CD4 TM domain followed by PS1 C-terminal fragment corresponding to the exact C37 region in our study (Kaether *et al.* 2004), strongly suggested that the C37 region has the domain(s) for the binding of NCT and APH-1. All results are summarized in Table 1.

Discussion

Although several lines of evidence have established the notion that PEN-2, APH-1 and NCT, in addition to PS, are required for the formation of the active γ-secretase complex (Francis *et al.* 2002; Edbauer *et al.* 2003; Kimberly *et al.* 2003; Takasugi *et al.* 2003), it remains unclarified how these three PS cofactors activate γ-secretase. To gain deep insights into the mechanism underlying the formation of the active γ-secretase complex, we reconstituted γ-secretase activity in PS-null cells by the co-expression of C-terminal truncated PS1 and the PS1 C-terminal short fragment. Using this reconstitution system, we found that both PS1 TM8 and the PS1 C-terminal last seven-amino-acid-residue tail are critical for γ-secretase activity and the assembly of the PS1 complex with APH-1 and NCT.

The PS C-terminal tail includes a hydrophobic stretch, which is a potential domain for the interaction with some proteins such as PDZ-domain-containing proteins (Saras *et al.* 1997; Tomita *et al.* 1999). Previously, it was pointed out that the PS C-terminal tail is important for PS endoproteolysis and PS stabilization (Tomita *et al.* 1999; Shirotani *et al.* 2000). Recently, it has also been shown that a short deletion of the C-terminal region from PS1 causes marked impairments in PS1 endoproteolysis and γ-secretase activity in PS-null cells (Bergman *et al.* 2004), indicating that the PS1 C-terminal region is critical for γ-secretase activity. However, it is not precisely known whether the PS C-terminal region is a functional domain for the formation of active γ-secretase or whether a short deletion at the C-terminus causes a conformational change leading to a loss of γ-secretase

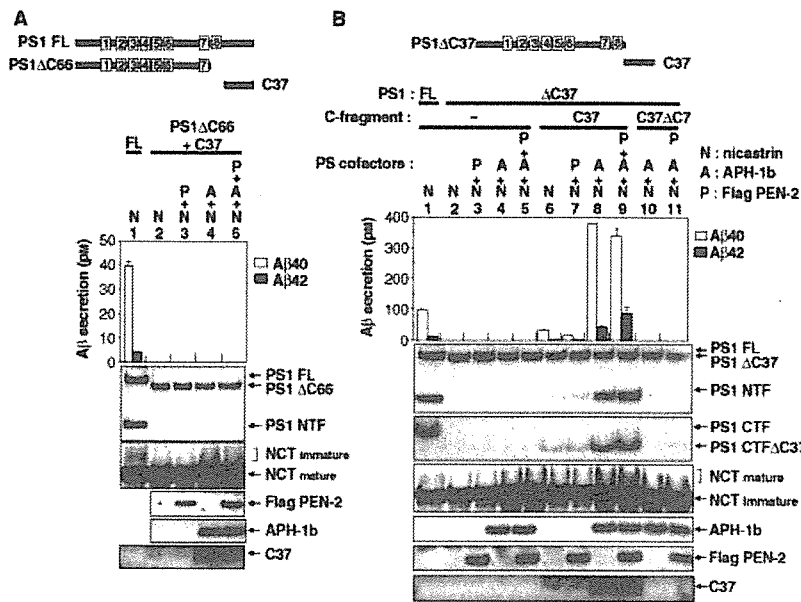


Figure 4 The rescue of a defect in γ -secretase activity of PS1 Δ C by the expression of PS1 C-terminal fragment with PS cofactors requires the PS1 TM8 region. After APP695 and the indicated exogenous PS cofactors were retrovirally expressed with (A) PS1 Δ C66 and C37 or (B) PS1 Δ C37 and C37 in PS null cells, A β secreted from these cells during a 48-h culture was quantified by ELISA, and CHAPSO-solubilized lysate (10 μ g) was immunoblotted with the anti-PS1 NTF antibody (for detection of PS1 FL and PS1 Δ C37), anti-PS1 loop antibody (for detection of PS1 CTF and PS1 CTF Δ C37), anti-APH-1b antibody, anti-FLAG antibody (for the detection of PEN-2), and the PS-C3 antibody (for detection of C37; note: this antibody does not immunoreact with C37 Δ C7). -, mock transfection (pMX). Values are means \pm SD of two independent dishes ($n = 2$). Data are representative of three independent experiments. The difference in A β level from PS1 FL between A and B is due to the difference in virus titer used for transfection.

activity. The successful reconstitution of γ -secretase activity in PS-null cells by the co-expression of C-terminally truncated PS1 and the PS1 C-terminal short fragment demonstrated that the PS1 C-terminal region has a distinct functional domain for the formation of active γ -secretase, and enabled us to investigate its role in γ -secretase activity.

PS1 Δ C66 has two aspartate residues in TM6 and TM7, which are essential for γ -secretase activity, but PS1 Δ C66 lacks the entire C-terminal region, including TM8 and the region immediately downstream from TM8. PS1 Δ C66 exhibited the complete loss of γ -secretase activity and endoproteolysis in PS-null cells; however, we found that the exogenous expression of a C-terminal fragment starting from TM8, that is, C68, completely rescued these defects when APH-1 and NCT were co-expressed. The limiting factors for γ -secretase activity in this reconstitution system were found to be APH-1 and NCT, not PEN-2 (Fig. 2C), and the restored endogenous expression level of PEN-2 is sufficient to reconstitute the γ -secretase activity of inactive PS1 Δ C66. Indeed, this interpretation was supported by our result showing that PS1 Δ C66 had a marked defect in the binding of NCT and APH-1, but PS1 Δ C66 did not have a significant defect in the binding of PEN-2. In addition, the rescue of γ -secretase activity was completely accompanied by a rescue of the defect in the assembly of PS1 Δ C66 with APH-1 and NCT. It was

also noted that these rescues were completely dependent on the presence of the C-terminal last seven-amino-acid-residue tail of C68. This result is completely consistent with the previous result showing that the extreme C-terminus of PS1 is essential for the assembly of active γ -secretase (Bergman *et al.* 2004). From these results, we concluded that the active γ -secretase complex is reconstituted by the exogenous co-expression of PS1 Δ C66, C68 and PS cofactors APH-1 and NCT.

Recently, it has been shown that the PS1 C-terminus is involved in the interaction with NCT and APH-1 (Bergman *et al.* 2004). We also showed that the association of C68 Δ C7 with PS1 Δ C66 and NCT was lower than that of C68 (Fig. 3B). Therefore, the failure of C68 lacking the C-terminal seven-amino acid residues (C68 Δ C7) to rescue the formation of the active γ -secretase complex was likely to be caused by the lower association of C68 Δ C7 with PS1 Δ C66 and NCT, and possibly with APH-1, than that of C68 (Fig. 3B).

PS endoproteolysis is not always associated with γ -secretase activity, because mutant PS1 Δ exon 9 is not endocleaved (Thinakaran *et al.* 1996). However, this mutant PS1 has γ -secretase activity (Wolfe *et al.* 1999). Therefore, the necessity of PS endoproteolysis for γ -secretase activity has not been firmly established. Our result also showed that the reconstituted γ -secretase activity induced by the truncated PS fragments is not associated with the extent of PS endoproteolysis

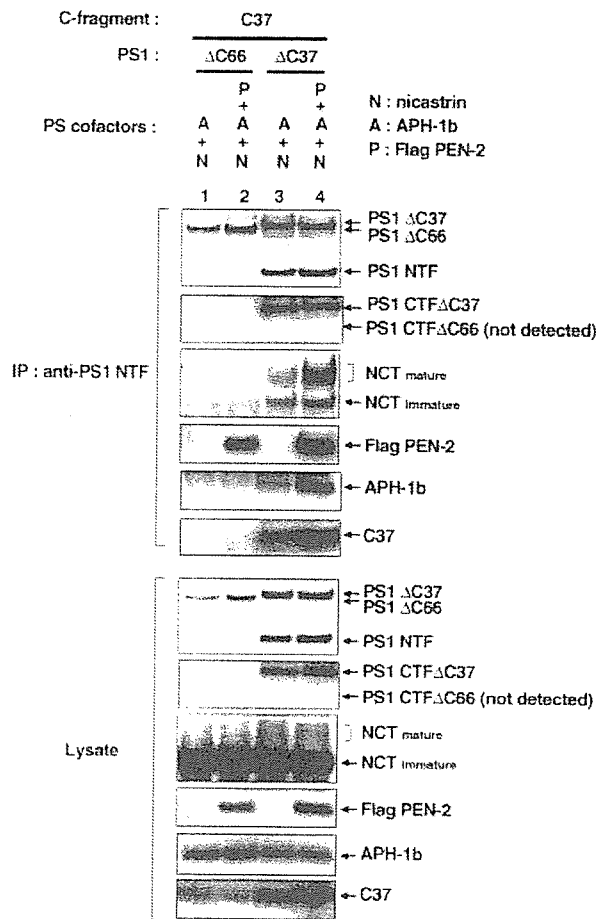


Figure 5 The assembly of the γ -secretase complex requires the PS1 TM8 region. After APP695 and the indicated exogenous PS cofactors were retrovirally expressed with PS1 Δ C66 and C37 or with PS1 Δ C37 and C37 in PS-null cells. CHAPSO-solubilized lysate (1 mg) was immunoprecipitated (IP) with the anti-PS1 NTF antibody (H-70) and then immunoblotted (IB) with the anti-PS1 NTF antibody (Chemicon International, Inc.; for detection of PS1 Δ C37, PS1 Δ C66 and PS1 NTF), anti-PS1 loop monoclonal antibody (for detection of PS1 CTF Δ C37), anti-APH-1b antibody, anti-FLAG antibody, anti-NCT antibody and PS-C3 antibody (for detection of C37). CHAPSO-solubilized lysate (10 μ g) was also immunoblotted with the same antibodies (the bottom four panels). Data are representative of two independent experiments. Note: PS1 NTF and PS1 CTF Δ C66 in lanes 1 and 2 were not detected, because the expression of PS1 Δ C66 with C37 and PS cofactors did not cause the endoproteolysis of PS1 Δ C66.


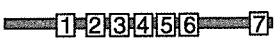
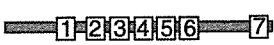


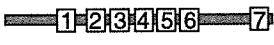

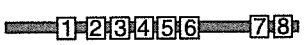


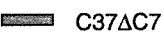
although the stimulation of PS Δ C endoproteolysis by the expression of exogenous PEN-2 was observed in this reconstitution system (Figs 2A, 3A, and 4B). In addition, the reconstituted γ -secretase activity by the truncated PS

fragments was dependent on APH-1 level, while γ -secretase activity from FL PS1 is not dependent on the APH-1 level (Supplementary Fig. S2). At present, we do not know the exact reason for the difference in the exogenous PS cofactors required for the stimulation of γ -secretase activity between the expression of PS FL and that of the truncated PS fragments. One possible explanation is that PS FL requires PS endoproteolysis for the conformational change from an inactive form to an active form, and this step is the limiting step for the activation of PS FL; however, the truncated PS fragments might not require PS endoproteolysis for forming the active complex, probably because the complex of the truncated PS fragments has a lower structural integrity than that of the PS FL. Instead, the truncated PS fragments required APH-1 and NCT rather than the stimulation of PS endoproteolysis by PEN-2 expression for the proper conformation and/or the proper trafficking of the complex for reconstituted γ -secretase activity. The difference in the structural integrity could also generate the difference in γ -secretase activity between the PS complex and the complex reconstituted by the truncated PS fragments, as observed in this study.

As previously reported (Herreman *et al.* 2003; Nyabi *et al.* 2003), the maturation of NCT is separable from γ -secretase activity, strongly suggesting that the difference in the extent of maturation of NCT in the reconstituted truncated PS complex is unknown, we speculate that the intracellular site, where the assembly of truncated PS fragments with PS cofactors occurs, may be slightly different from the case of wild-type (wt) PS, because PS that lacks the C-terminal portion does not reside in the ER as previously reported (Kaether *et al.* 2004), whereas full-length PS resides in the ER. The assembly of full-length wt PS with PS cofactors is likely to occur in the ER (Capell *et al.* 2005; Niimura *et al.* 2005), which is followed by the transport of the complex into the Golgi compartment, where the terminal sugar modification of NCT occurs. However, if the truncated PS fragments and the over-expressed immature NCT exist in the distal/post-Golgi compartment, they form the active γ -secretase complex; the glycosylation of NCT in the complex could be less than that in the wt PS complex.

To determine whether the TM8 of C68 is required for the rescue of a defect in the γ -secretase activity of PS1 Δ C66, we investigated whether the C37 fragment, which is immediately downstream of TM8 and therefore

Table 1 Summary of functional rescue of C68 and C37 for inactive PS1 Δ C in PS-null cells

| | Transgene (+ exogenous three PS cofactors) | γ -secretase activity | Assembly of PS1 Δ C with | | |
|---|--|--|---------------------------------|-------|-------|
| | | | NCT | APH-1 | PEN-2 |
| 1 | PS1 FL  | + | + | + | + |
| 2 | PS1 Δ C66  | - | - | - | + |
| 3 | PS1 Δ C66   C68 | + | + | + | + |
| | |  C68 Δ C7 | - | - | - |
| 4 | PS1 Δ C66   C37 | - | - | - | + |
| 5 | PS1 Δ C37  | - | - | - | + |
| 6 | PS1 Δ C37   C37 | + | + | + | + |
| | |  C37 Δ C7 | - | * - | * - |

1, 2 and 3, summary of the results of Figs 2 and 3; 4, 5 and 6, summary of the results of Figs 4 and 5. +, rescued; -, not rescued; * data not shown.

lacks TM8, can similarly rescue a defect in the γ -secretase activity of PS1 Δ C66. The result showed a failure of the rescue; however, the expression of C37 with APH-1 and NCT rescued a defect in the γ -secretase activity of PS1 Δ C37 that has TM8, but lacks the C-terminal region immediately downstream of TM8. These results clearly demonstrate that TM8 is involved in the formation of an active γ -secretase. Indeed, C37 expression did not rescue a defect in the assembly of PS1 Δ C66 with NCT and APH-1, but it significantly rescued a defect in the assembly of PS1 Δ C37 with NCT and APH-1, indicating that TM8 is involved in the assembly of PS1 Δ C37 with NCT and APH-1. Thus, we concluded that TM8 is also required for the formation of an active PS1 complex with NCT and APH-1 (Table 1).

Previously, it was shown that the TM of NCT is involved in the assembly of an active γ -secretase complex, and that the cytoplasmic domain of NCT is dispensable for γ -secretase complex formation (Capell *et al.* 2003). It was also shown that the GXXXG motif in the TM of APH-1 is critical for the assembly of the γ -secretase complex (Lee *et al.* 2004), strongly suggesting that the TM of APH-1 is involved in the assembly of this

complex. Taken together with our results, the TM8 of PS1 is likely to interact with NCT or APH-1 or both through their transmembrane. In addition, our data also demonstrate that the PS1 C-terminal seven-amino-acid-residue tail is critical for the assembly of the γ -secretase complex in the reconstitution system (Table 1). A previous study has shown that the PS1 C-terminus probably binds to the TM of NCT (Kaether *et al.* 2004). Therefore, both the C-terminus and PS1 TM8 appear to bind to the TM of NCT. Although C68 and C37 are likely to have the domains for the interaction of NCT and APH-1 (Supplementary Fig. S1; Kaether *et al.* 2004), how the TM8 in concert with C-terminus interact with NCT and APH-1 to form the active PS complex remains to be determined in future studies. The formation of an intermediate subcomplex of APH-1 and NCT as previously shown (LaVoie *et al.* 2003) also could be a prerequisite for the interaction of PS TM8 and the C-terminus with APH-1/NCT.

Because the proposed catalytic aspartate residues are embedded in TM6 and TM7, it remains to be clarified how hydrolysis that is required for γ -secretase activity occurs within the hydrophobic environment. Interestingly,

recent studies have shown the possibility that PS has a ninth TM in the C-terminal region (Henricson *et al.* 2005; Laudon *et al.* 2005). If this is the case, the C37 in our study is supposed to harbor the novel TM9. Although, at present, the precise roles of the TM8 and possibly also TM9 are unknown, one possible role is that the C-terminal TM(s) contribute to the formation of the catalytic space between TM6 and TM7 within the hydrophobic environment of the lipid bilayer, because these TM(s) are found to be necessary for γ -secretase activity and the association with APH-1/NCT, that are the essential cofactors for γ -secretase activity.

In this study, we established the reconstitution of γ -secretase activity by truncated PS fragments and PS cofactors. With this reconstitution system, we demonstrated that both PS1 TM8 and the PS1 C-terminal last-seven-amino-acid-residue tail are critical for γ -secretase activity and the assembly of the PS1 complex with APH-1 and NCT. More precise studies of how TM8 and the C-terminal tail are involved in the assembly of the γ -secretase complex may help clarify the regulation of γ -secretase activity.

Experimental procedures

Antibodies, reagents and cell lines

The monoclonal antibody 6E10 specific to human A β 1-17 was purchased from Senetek (St. Louis, MO, USA). The other A β antibodies have all been characterized previously (Asami-Odaka *et al.* 1995). The anti-APP N-terminal antibody 22C11 was purchased from Sigma (St. Louis, MO, USA). A rat anti-PS1 antibody (for NTF of PS1) and a mouse anti-PS1 loop monoclonal antibody were purchased from Chemicon International, Inc. (Temecula, CA, USA). A goat anti-PS1 C-20 antibody (for PS1 C-terminal 20 amino acid residues) and a rabbit anti-PS1 H-70 antibody (for PS1 N-terminal 70 amino acid residues) were purchased from Santa Cruz Biotechnology, Inc. A rabbit PS-C3 antibody was prepared against the synthetic peptide corresponding to the C-terminal 15 amino acid residues of PS1. An anti-FLAG antibody was purchased from Sigma. A rabbit anti-human APH-1b antibody was prepared against the synthetic peptide corresponding to the C-terminal 17 amino acid residues of APH-1b. An anti-nicastrin antibody was purchased from Sigma. A rabbit anti-PEN-2 antibody (for the detection of the endogenous PEN-2) was purchased from Zymed Laboratory Inc. PS1/PS2 double-deficient murine fibroblasts (PS-null cells) and wild-type murine fibroblasts immortalized with a large T antigen were maintained as previously described (Herreman *et al.* 2000; Sai *et al.* 2002).

Plasmids and retrovirus-mediated gene expression

cDNAs encoding PS1 Δ C were generated from pMX-PS1 by the PCR method. The primer sequences used for the PCR were as

follows: a sense primer: 5'-TGCAGAATTCATGACAGAGT-TACCTGCA-3'; and anti-sense primers: 5'-CATGCTCGAGT-CATTTCTTGAAAATGGCAAGGAG-3' (PS1 Δ C37: the last 37 amino acids deletion), and 5'-CATGCTCGAGTCAACT-GGCTGTTGCTGAGGCTT-3' (PS1 Δ C66: the last 66 amino acids deletion). The PCR products were digested with *Eco*RI and *Xho*I inserted into pMX (Onishi *et al.* 1996). cDNA encoding PS1 C-terminal 37 (C37: residues 431-467) or 68 (C68: residues 400-467) amino acid residues starting at Met, which was added by the *Eco*RI site followed by Kozak consensus sequence at the 5' end and the *Xho*I site at the 3' end was generated by the PCR method using the following primers: sense primers, 5'-TGCA-GAATTCACCATGGCATTGCCAGCTCTTCCA-3' (C37) and 5'-TGCAGAATTCACCATGGCCAGTGGAGACTGGAAC-3' (C68); and an anti-sense primer, 5'-CATGCTCGAGCTAGATATAAAATTGATGG-3'. The resultant cDNAs were inserted into pMX at *Eco*RI and *Xho*I. cDNAs encoding C37 Δ C7 and C68 Δ C7 were generated by the PCR method using the following primers: a sense primer for C37 or C68; and an anti-sense primer: 5'-CATGCTCGAGCTATAATTGGTCCATAAAAAGGCTG-3'. The resultant cDNAs were inserted into pMX at *Eco*RI and *Xho*I.

pMX-F-PEN-2 is a *Bam*HI-*Sal*I fragment carrying the sequence encoding the N-terminal FLAG-tagged PEN-2 and Kozak consensus sequence (CCACC) at the 5' end of FLAG-PEN-2 inserted into the *Bam*HI and *Sal*I sites of pMX as previously described (Shiraishi *et al.* 2004). pMX-NCT, pMX-PS1, and pMX-APP695 were constructed as previously described (Komano *et al.* 2002). APH-1b (Francis *et al.* 2002) was generated from the cDNA library prepared from HEK293 cells using a sense primer, GCGAATTCCTTCCGCGGTGGCCATGACT and anti-sense primer, GCAGATCTGAAGTGTGGTTCCCTGAGG. The PCR product was digested with *Eco*RI and inserted into pMX at the *Eco*RI site.

All resulting constructs were verified by DNA sequencing. Retrovirus-mediated gene expression in cells was carried out as previously reported (Onishi *et al.* 1996; Komano *et al.* 2002). The infection efficiency was nearly 100% in this study, as estimated in a control experiment using pMX-GFP (retroviral vector carrying GFP).

A β detection and co-immunoprecipitation techniques

A β level was determined by ELISA as previously described (Asami-Odaka *et al.* 1995). The capture antibody used was BNT77. The detector antibodies used were horseradish peroxidase (HRP)-conjugated BA27 (for A β 40) and HRP-conjugated BC05 (for A β 42). ELISA data were statistically analyzed by ANOVA using StatView-J.4.11 (Abacus Concepts, Inc., Berkeley, CA, USA). Cultured cells were lysed in 1% CHAPSO buffer [1% CHAPSO, 150 mM NaCl, 10 mM Tris/HCl (pH 7.5), 2 mM EDTA, a protease inhibitor cocktail]. CHAPSO-solubilized proteins were co-immunoprecipitated with PS1 by incubating with the anti-PS1 NTF antibody and 100 μ L of 20% protein-G Sepharose (Pharmacia) slurry with rotation at 4 $^{\circ}$ C overnight, as

previously described (Sudoh *et al.* 1998; Li *et al.* 2000a). The immunoprecipitates were solubilized in SDS sample buffer (0.0625 M Tris-HCl (pH 6.8), 2% SDS, 10% glycerol, 5% 2-mercaptoethanol, and 8 M urea) and subjected to SDS-PAGE.

Acknowledgements

This study was supported by the Program for the Promotion of Fundamental Studies in Health Sciences of the Organization for Pharmaceutical Safety and Research; by a Grant-in-Aid for Scientific Research on Priority Areas (C)-Advanced Brain Science Project (to K.Y.); by a Grant-in-Aid 15659023 and 16390029 from the Ministry of Education, Culture, Sports, Sciences and Technology; by a grant from the Takeda Medical Research Foundation; by a Grant for Dementia and Bone Fracture from the Ministry of Health, Labor and Welfare, Japan. We thank Dr B. De Strooper (Katholieke Universiteit Leuven and Flanders Interuniversity, Herestraat, Belgium) for providing PS1/PS2 double-deficient fibroblasts and wild-type fibroblasts.

References

- Araki, Y., Miyagi, N., Kato, N., *et al.* (2004) Coordinated metabolism of Alcadin and amyloid β -protein precursor regulates FE65-dependent gene transactivation. *J. Biol. Chem.* **279**, 24343–24354.
- Asami-Odaka, A., Ishibashi, Y., Kikuchi, T., Kitada, C. & Suzuki, N. (1995) Long amyloid β -protein secreted from wild-type human neuroblastoma IMR-32 cells. *Biochemistry* **34**, 10272–10278.
- Bergman, A., Laudon, H., Winblad, B., Lundkvist, J. & Naslund, J. (2004) The extreme C terminus of presenilin 1 is essential for γ -secretase complex assembly and activity. *J. Biol. Chem.* **279**, 45564–45572.
- Capell, A., Beher, D., Prokop, S., *et al.* (2005) γ -secretase complex assembly within the early secretory pathway. *J. Biol. Chem.* **280**, 6471–6478.
- Capell, A., Kaether, C., Edbauer, D., *et al.* (2003) Nicastrin interacts with γ -secretase complex components via the N-terminal part of its transmembrane domain. *J. Biol. Chem.* **278**, 52519–52523.
- De Strooper, B. (2003) Aph-1, Pen-2, and Nicastrin with Presenilin generate an active γ -Secretase complex. *Neuron* **38**, 9–12.
- De Strooper, B., Saftig, P., Craessaerts, K., *et al.* (1998) Deficiency of presenilin-1 inhibits the normal cleavage of amyloid precursor protein. *Nature* **391**, 387–390.
- Edbauer, D., Winkler, E., Regula, J.T., Pesold, B., Steiner, H. & Haass, C. (2003) Reconstitution of γ -secretase activity. *Nature Cell Biol.* **5**, 486–488.
- Francis, R., McGrath, G., Zhang, J., *et al.* (2002) aph-1 and pen-2 are required for Notch pathway signaling, gamma-secretase cleavage of betaAPP, and presenilin protein accumulation. *Dev. Cell* **3**, 85–97.
- Henricson, A., Kall, L. & Sonnhhammer, E.L. (2005) A novel transmembrane topology of presenilin based on reconciling experimental and computational evidence. *FEBS J.* **272**, 2727–2737.
- Herreman, A., Serneels, L., Annaert, W., Collen, D., Schoonjans, L. & De Strooper, B. (2000) Total inactivation of γ -secretase activity in presenilin-deficient embryonic stem cells. *Nature Cell Biol.* **2**, 461–462.
- Herreman, A., Van Gassen, G., Bentahir, M., *et al.* (2003) γ -Secretase activity requires the presenilin-dependent trafficking of nicastrin through the Golgi apparatus but not its complex glycosylation. *J. Cell Sci.* **116**, 1127–1136.
- Kaether, C., Capell, A., Edbauer, D., *et al.* (2004) The presenilin C-terminus is required for ER-retention, nicastrin-binding and gamma-secretase activity. *EMBO J.* **23**, 4738–4748.
- Kimberly, W.T., LaVoie, M.J., Ostaszewski, B.L., Ye, W., Wolfe, M.S. & Selkoe, D.J. (2003) γ -secretase is a membrane protein complex comprised of presenilin, nicastrin, Aph-1, and Pen-2. *Proc. Natl. Acad. Sci. USA* **100**, 6382–6387.
- Komano, H., Shiraishi, H., Kawamura, Y., *et al.* (2002) A new functional screening system for identification of regulators for the generation of amyloid β -protein. *J. Biol. Chem.* **277**, 39627–39633.
- Laudon, H., Hasson, E.M., Melen, K., *et al.* (2005) A nine transmembrane domain topology for presenilin 1. *J. Biol. Chem.* **280**, 35352–35360.
- Laudon, H., Mathews, P.M., Karlstrom, H., *et al.* (2004) Co-expressed presenilin 1 NTF and CTF form functional γ -secretase complexes in cells devoid of full-length protein. *J. Neurochem.* **89**, 44–53.
- LaVoie, M.J., Fraering, P.C., Ostaszewski, B.L., *et al.* (2003) Assembly of the γ -secretase complex involves early formation of an intermediate subcomplex of Aph-1 and nicastrin. *J. Biol. Chem.* **278**, 37213–37222.
- Lee, S.F., Shah, S., Yu, C., *et al.* (2004) A conserved GXXXG motif in APH-1 is critical for assembly and activity of the γ -secretase complex. *J. Biol. Chem.* **279**, 4144–4152.
- Li, X. & Greenwald, I. (1998) Additional evidence for an eight-transmembrane-domain topology for *Caenorhabditis elegans* and human presenilins. *Proc. Natl. Acad. Sci. USA* **95**, 7109–7114.
- Li, Y.M., Lai, M.T., Xu, M., *et al.* (2000a) Presenilin 1 is linked with γ -secretase activity in the detergent solubilized state. *Proc. Natl. Acad. Sci. USA* **97**, 6138–6143.
- Li, Y.M., Xu, M., Lai, M.T., *et al.* (2000b) Photoactivated γ -secretase inhibitors directed to the active site covalently label presenilin 1. *Nature* **405**, 689–694.
- Niimura, M., Isoo, N., Takasugi, N., *et al.* (2005) Aph-1 contributes to the stabilization and trafficking of the γ -secretase complex through mechanisms involving inter- and intramolecular interactions. *J. Biol. Chem.* **280**, 12967–12975.
- Nyabi, O., Bentahir, M., Horre, K., *et al.* (2003) Presenilins mutated at Asp-257 or Asp-385 restore Pen-2 expression and Nicastrin glycosylation but remain catalytically inactive in the absence of wild type Presenilin. *J. Biol. Chem.* **278**, 43430–43436.
- Onishi, M., Kinoshita, S., Morikawa, Y., *et al.* (1996) Applications of retrovirus-mediated expression cloning. *Exp. Hematol.* **24**, 324–329.
- Ratovitski, T., Slunt, H.H., Thinakaran, G., Price, D.L., Sisodia, S.S. & Borchelt, D.R. (1997) Endoproteolytic processing and stabilization of wild-type and mutant presenilin. *J. Biol. Chem.* **272**, 24536–24541.

- Sai, X., Kawamura, Y., Kokame, K., *et al.* (2002) Endoplasmic reticulum stress-inducible protein, Herp, enhances presenilin-mediated generation of amyloid β -protein. *J. Biol. Chem.* **277**, 12915–12920.
- Saras, J., Engstrom, U., Gonez, L.J. & Heldin, C.H. (1997) Characterization of the interactions between PDZ domains of the protein-tyrosine phosphatase PTPL1 and the carboxyl-terminal tail of Fas. *J. Biol. Chem.* **272**, 20979–20981.
- Selkoe, D.J. (2001) Alzheimer's disease: genes, proteins, and therapy. *Physiol. Rev.* **81**, 741–766.
- Shiraishi, H., Sai, X., Wang, H.Q., *et al.* (2004) PEN-2 enhances gamma-cleavage after presenilin heterodimer formation. *J. Neurochem.* **90**, 1402–1413.
- Shirovani, K., Takahashi, K., Araki, W., Maruyama, K. & Tabira, T. (2000) Mutational analysis of intrinsic regions of presenilin 2 that determine its endoproteolytic cleavage and pathological function. *J. Biol. Chem.* **275**, 3681–3686.
- Steiner, H., Kostka, M., Romig, H., *et al.* (2000) Glycine 384 is required for presenilin-1 function and is conserved in bacterial polytopic aspartyl proteases. *Nature Cell Biol.* **2**, 848–851.
- Sudoh, S., Kawamura, Y., Sato, S., *et al.* (1998) Presenilin 1 mutations linked to familial Alzheimer's disease increase the intracellular levels of amyloid β -protein 1–42 and its N-terminally truncated variant(s) which are generated at distinct sites. *J. Neurochem.* **71**, 1535–1543.
- Takasugi, N., Tomita, T., Hayashi, I., *et al.* (2003) The role of presenilin cofactors in the γ -secretase complex. *Nature* **422**, 438–441.
- Thinakaran, G., Borchelt, D.R., Lee, M.K., *et al.* (1996) Endoproteolysis of presenilin 1 and accumulation of processed derivatives in vivo. *Neuron* **17**, 181–190.
- Thinakaran, G., Harris, C.L., Ratovitski, T., *et al.* (1997) Evidence that levels of presenilins (PS1 and PS2) are coordinately regulated by competition for limiting cellular factors. *J. Biol. Chem.* **272**, 28415–28422.
- Tomita, T., Takikawa, R., Koyama, A., *et al.* (1999) C terminus of presenilin is required for overproduction of amyloidogenic A β 42 through stabilization and endoproteolysis of presenilin. *J. Neurosci.* **19**, 10627–10634.
- Tomita, T., Watabiki, T., Takikawa, R., *et al.* (2001) The first proline of PALP motif at the C terminus of presenilins is obligatory for stabilization, complex formation, and gamma-secretase activities of presenilins. *J. Biol. Chem.* **276**, 33273–33281.
- Weihofen, A., Binns, K., Lemberg, M.K., Ashman, K. & Martoglio, B. (2002) Identification of signal peptide peptidase, a presenilin-type aspartic protease. *Science* **296**, 2215–2218.
- Wolfe, M.S., Xia, W., Ostaszewski, B.L., Diehl, T.S., Kimberly, W.T. & Selkoe, D.J. (1999) Two transmembrane aspartates in presenilin-1 required for presenilin endoproteolysis and γ -secretase activity. *Nature* **398**, 513–517.

Received: 2 August 2005

Accepted: 3 October 2005

Supplementary material

The following supplementary material is available for this article online:

Figure S1 Interaction of C68 with NCT and APH-1

Figure S2 A β generation in PS-null cells expressing truncated PS fragments is APH-1-dependently increased

Formation of Tau Inclusions in Knock-in Mice with Familial Alzheimer Disease (FAD) Mutation of Presenilin 1 (PS1)*

Received for publication, August 19, 2005, and in revised form, December 21, 2005. Published, JBC Papers in Press, December 23, 2005, DOI 10.1074/jbc.M509145200

Kentaro Tanemura[‡], Du-Hua Chui^{‡1}, Tetsuya Fukuda[‡], Miyuki Murayama[‡], Jung-Mi Park[‡], Takumi Akagi[§], Yoshitaka Tatebayashi[‡], Tomohiro Miyasaka[‡], Tetsuya Kimura[‡], Tsutomu Hashikawa[§], Yuka Nakano[¶], Takashi Kudo[¶], Masatoshi Takeda[¶], and Akihiko Takashima^{‡2}

From the [‡]Laboratory for Alzheimer Disease and [§]Neural Architecture, Brain Science Institute, RIKEN, Wako, Saitama 351-0198, Japan and the [¶]Department of Psychiatry and Behavioral Science and Environmental Medicine, Osaka University Graduate School of Medicine, 2-2 Yamadaoka, Suita, Osaka 565-0871, Japan

Mutations in the presenilin 1 (PS1) gene are responsible for the early onset of familial Alzheimer disease (FAD). Accumulating evidence shows that PS1 is involved in γ -secretase activity and that FAD-associated mutations of PS1 commonly accelerate $A\beta_{1-42}$ production, which causes Alzheimer disease (AD). Recent studies suggest, however, that PS1 is involved not only in $A\beta$ production but also in other processes that lead to neurodegeneration. To better understand the causes of neurodegeneration linked to the PS1 mutation, we analyzed the development of tau pathology, another key feature of AD, in PS1 knock-in mice. Hippocampal samples taken from FAD mutant (I213T) PS1 knock-in mice contained hyperphosphorylated tau that reacted with various phosphodependent tau antibodies and with Alz50, which recognizes the conformational change of PHF tau. Some neurons exhibited Congo red birefringence and Thioflavin T reactivity, both of which are histological criteria for neurofibrillary tangles (NFTs). Biochemical analysis of the samples revealed SDS-insoluble tau, which under electron microscopy examination, resembled tau fibrils. These results indicate that our mutant PS1 knock-in mice exhibited NFT-like tau pathology in the absence of $A\beta$ deposition, suggesting that PS1 mutations contribute to the onset of AD not only by enhancing $A\beta_{1-42}$ production but by also accelerating the formation and accumulation of filamentous tau.

Alzheimer disease (AD)³ is characterized pathologically by neurofibrillary tangles (NFTs), which are composed of highly phosphorylated tau, and by neuronal loss and $A\beta$ deposition. AD is manifested symptomatically by dementia. Presenilin 1 (PS1), a gene identified to be responsible, in part, for early onset familial Alzheimer disease (FAD), has been cloned (1, 2). To date more than 70 mutations of the PS1 gene have been reported (3, 4). In each mutation, early onset of AD develops with 100% penetration (3, 4). PS1 is required for γ -secretase to cleave amyloid precursor protein into $A\beta$ species such as $A\beta_{1-40}$ and $A\beta_{1-42}$.

Improper cleavage of amyloid precursor protein because of a PS1 mutation increases the production of $A\beta_{1-42}$ (5–7), a highly aggregative, neurotoxic species of $A\beta$ that is longer than the less toxic $A\beta_{1-40}$. One hypothesis for the neurodegeneration observed in AD, therefore, is that PS1 mutation leads to increasing amounts of extracellular, neurotoxic $A\beta_{1-42}$, thereby inducing neurodegeneration (8–11).

Accumulating data suggest that, in addition to its role in $A\beta_{1-42}$ production, PS1 mutation also contributes to NFT formation. For example, PS1 conditional knock-out mice display phosphorylated tau, synaptic dysfunction, and memory impairment, even in the absence of $A\beta$ production and deposition (12). In a related line of research, some patients clinically diagnosed with fronto-temporal dementia (FTD) have been shown to harbor PS1 mutations (13–16). Interestingly, FTD is characterized by the appearance of NFTs without $A\beta$ deposition (17). A patient harboring the G183V PS1 mutation displayed the clinical manifestations of FTD and exhibited phospho-tau-positive Pick body pathology throughout the cortex and limbic region, without $A\beta$ deposition. Other reports have also shown that PS1 mutations accelerate NFT formation and neuronal loss without affecting the rate of $A\beta$ deposition (18). Thus, these data lead to the hypothesis that PS1 mutations might contribute to NFT formation as well as increase $A\beta_{1-42}$ production in FAD.

To investigate this hypothesis, we examined tau pathology in mutant PS1 I213T knock-in mice (19). This line of mice was generated with a targeted insertion of the I213T missense mutation into exon 7 of the mouse PS1 gene using homologous recombination. Therefore, these PS1 mutant knock-in mice harbor the FAD mutation in the mouse PS1 gene and produce PS1 I213T. Heterozygote mutant PS1 I213T mice showed no change in $A\beta_{1-40}$ levels but had increased levels of $A\beta_{1-42}$, a 1.3-fold increase when compared with wild-type mice. This $A\beta_{1-42}$ increase is comparable to that observed in human cases. Because this mouse strain shares the same PS1 genotype and related pathology as that of patients harboring the PS1 mutation, we initially expected these mice to develop the AD phenotype. The increase in murine $A\beta_{1-42}$, however, failed to lead to a corresponding $A\beta$ deposition, possibly because murine $A\beta$ has a different amino acid sequence that reduces its tendency to aggregate. Using this dissociation to our advantage, we investigated the $A\beta$ deposition-independent effects of the PS1 mutation in this mouse model. We found that GSK-3 β activation was followed by the accumulation of hyperphosphorylated tau in the hippocampal region, which fulfills the histological criteria for the presence of NFTs.

EXPERIMENTAL PROCEDURES

Animals—Mutant PS1 I213T knock-in mice (mPS1 mice) were maintained at the RIKEN BSI animal facilities according to the Institute guidelines for the treatment of experimental animals.

* This work was supported in part by a grant from the Ministry of Education, Science, Sports, and Culture of Japan. The costs of publication of this article were defrayed in part by the payment of page charges. This article must therefore be hereby marked "advertisement" in accordance with 18 U.S.C. Section 1734 solely to indicate this fact.

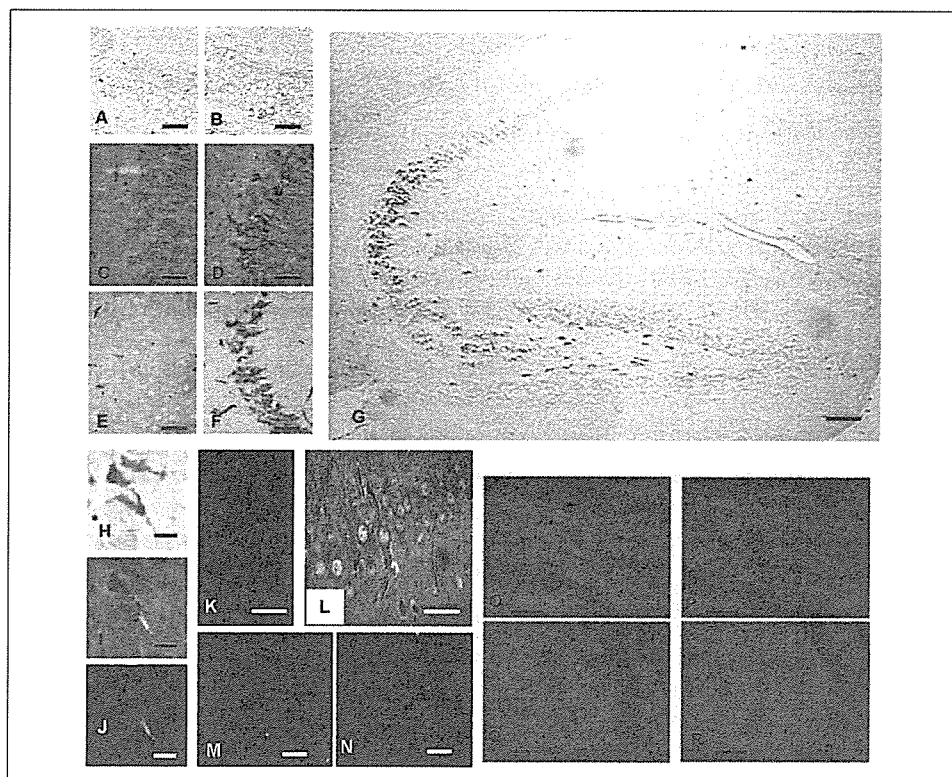
¹ Present address: Neuroscience Research Institute, Peking University, 38 Xue Yuan Rd., Beijing 100083, China.

² To whom correspondence should be addressed: Laboratory for Alzheimer Disease, RIKEN Brain Science Institute, 2-1 Hirosawa, Wako-shi, Saitama 351-0198, Japan. Tel.: 81-48-467-9632; Fax: 81-48-467-5916; E-mail: kenneth@brain.riken.jp.

³ The abbreviations used are: AD, Alzheimer disease; PS1, presenilin 1; FAD, familial Alzheimer disease; $A\beta$, amyloid β protein; NFT, neurofibrillary tangles; FTD, fronto-temporal dementia; GSK-3 β , glycogen synthase kinase-3 β ; PHFs, paired helical filaments; TBS, Tris-buffered saline; CDK5, cyclin-dependent kinase 5; JNK, c-Jun N-terminal kinase; MAP, mitogen-activated protein; TUNEL, terminal deoxynucleotidyltransferase-mediated dUTP nick end-labeling; RIPA, radioimmune precipitation assay buffer.

Tau Inclusions in FAD Mutant PS1 Knock-in Mice

FIGURE 1. Histochemical and histopathological assessment of brain sections from wild-type (wPS1) and mutant PS1 knock-in (mPS1) mice. A–G, anti-tau immunoreactivity in hippocampal CA3 of wPS1 mice (A, C, E) and heterozygous mPS1 mice (B, D, F) at 7 months (A, B) and 15 months (C–G) of age. A–D, PS199 immunoreactivity; E–G, Alz50 immunoreactivity. The low power micrograph in G shows how hippocampal immunoreactivity is confined largely to CA3. H–L, histopathology in CA3 of heterozygous mPS1 mice at 15 months of age. H–J, Congo red staining without (H) or with (I, J) polarizing filters; K, Thioflavin T; and L, Gallyas silver-staining. M and N, immunoreactivity in CA3 of wPS1 (M) and heterozygous mPS1 mice (N) at 16 months of age. M and N, double immunolabeling with α -tubulin (red) and PS199 (green) antibodies. O, TUNEL staining of dentate gyrus in the wPS1 mouse; P, TUNEL staining of dentate gyrus in the homozygous mPS1 mouse; Q, TUNEL staining of CA3 in the wPS1 mouse; R, TUNEL staining of CA3 in the homozygous mPS1 mouse. Scale bars: 50 μ m in A–F and O–R; 100 μ m in G; 10 μ m in H–L; 25 μ m in M and N.



Antibodies—The following antibodies were used: mouse monoclonal anti-tubulin (DM1A, Sigma); anti-ubiquitin (Santa Cruz Biotechnology); anti-GSK3 β (Transduction Laboratory); anti-MAP2 (HM2, Sigma); anti-tau Alz50, which recognizes the conformational epitope of paired helical filaments (PHFs), component of NFT (a generous gift from Dr. P. Davies, Albert Einstein College of Medicine, Bronx, NY); anti-phosphorylated tau AT8 (Innogenetics Zwijndrecht); anti-dephosphorylated tau, Tau-1 (Chemicon); rabbit polyclonal anti-tau JM (20); anti-phosphorylated tau PS199, PS262, PS396, PS404, and PS422 (BIO-SOURCE), which recognize tau phosphorylated at the indicated sites; and anti-GSK3 β Ser-9 (Cell Signaling).

Western Blot Analysis—Brains were homogenized in modified radioimmunoprecipitation assay (RIPA) buffer (50 mM Tris, 150 mM NaCl, 1% Nonidet P-40, 5 mM EDTA, 0.5% sodium deoxycholate, and 0.1% SDS, pH 8.0), and the suspension was centrifuged at 100,000 \times g for 20 min at 4 $^{\circ}$ C in an Optima TL ultracentrifuge (Beckman). The pellet was washed five times with 1% SDS-Tris-buffered saline (TBS) (50 mM Tris, 150 mM NaCl, and 1% SDS, pH 8.0) followed each time by centrifugation. The SDS-insoluble pellet was solubilized in 70% formic acid, lyophilized, reconstituted in Laemmli SDS-PAGE sample buffer, and subjected to SDS-PAGE. Separated proteins were blotted onto Immobilon-P membranes (Millipore). The membranes were incubated with primary antibody then with the species-appropriate horseradish peroxidase-conjugated secondary antibody. Immunoreactivity was visualized with a chemiluminescent detection system (ECL, Amersham Biosciences). Quantitation and visual analysis of immunoreactivity were performed with a computer-linked LAS-1000 Bio-Imaging Analyzer System (Fujifilm) using the software program Image Gauge 3.0 (Fujifilm).

Glycogen Synthase Kinase (GSK)-3 β Activity—Brains were homogenized in TBS (pH 7.4) and centrifuged at 100,000 \times g for 20 min at 4 $^{\circ}$ C in an Optima TL ultracentrifuge (Beckman). Protein concentration in

the supernatant was determined with a Bradford protein assay, and 10- μ g samples were assayed for GSK-3 β activity with an immunoprecipitation assay (21).

Ultrastructural Studies—For electron microscopy studies, SDS-insoluble materials were prepared from the brains of mPS1 mice as described above in the Western blot analysis section. The materials were mildly sonicated and dispersed in phosphate-buffered saline. The dispersed solution was absorbed onto glow-discharged supporting membranes on 400-mesh grids and prefixed by floating the grids on drops of 4% paraformaldehyde in 0.1 M phosphate buffer for 5 min. After washing, the grids were incubated with primary antibody (JM, anti-tau antibody), followed with a 5-nm colloidal gold-conjugated secondary antibody. The grids were then negatively stained with 2% sodium phosphotungstic acid, dried, and observed with a LEO 912AB electron microscope at 100 kV.

Immunohistochemical and Histopathological Studies—Brains were immersion-fixed in 10%-buffered formalin, and paraffin-embedded sections (4 μ m) were prepared. PS199, Alz50, anti-MAP2, and AT8 were used as primary antibodies. After reacting the sections with species-appropriate secondary antibodies, we visualized for light microscopy analyses immunoreactive elements by treating the sections with ABC followed by DAB using Peroxidase Stain DAB kits (Nacalai Tesque Japan). PS199 and anti- α -tubulin were used as primary antibodies for confocal laser microscopy analyses. Immunoreactive elements were visualized with Alexa568-conjugated anti-mouse IgG and Alexa488-conjugated anti-rabbit IgG, and then examined with a Radiance 2000 KR3 confocal microscope (Bio-Rad). We stained some sections with Congo red and Thioflavin T, which recognize the β -sheet structure of tau fibrils, and then examined them with a light microscope equipped with crossed polarizing filters (Nikon). NFTs were identified using a standard Gallyas silver-impregnation method, which is used to assess structural changes of the brain in AD (22).

RESULTS

The A β levels in the brains of mPS1 knock-in mice were quantified by sandwich enzyme-linked immunoassay (23) and Western blot analysis. Similar to a previous report (19), the level of A β_{1-42} was elevated in the brains of mPS1 mice compared with that in the brains of wild-type mice (wPS1 mice). Most of the A β_{1-40} and A β_{1-42} was recovered in the Triton X-100-soluble fraction, and very little was recovered in the 1% SDS-insoluble fraction, suggesting that neither A β_{1-40} nor A β_{1-42} aggregated and deposited within the brains of the mPS1 mice. Moreover, A β immunostaining in tissue sections was absent, suggesting again that neither extracellular nor intracellular A β accumulated *in vivo* (data not shown). Thus, murine A β failed to deposit in the brains of mPS1 mice, even though A β_{1-42} levels in these brains increased.

Characterization of NFT-like Pathology in Mutant PS1 Mice—Five-month-old heterozygous mPS1 mice exhibited no pathological changes (Fig. 1A); however, in 7-month-old or older mice, we detected phospho-tau accumulation (PS199) in neurons in the hippocampal region (Fig. 1B). The prevalence and distribution of these PS199-positive neurons gradually increased and widened, respectively, with age, and in 14–16-month-old mice, we observed phospho-tau immunoreactivity in hippocampal CA3 neurons (Fig. 1D). By contrast, wPS1 mice did not show this pattern of phospho-tau immunoreactivity (Fig. 1, C and D). Alz50, an antibody that recognizes the conformational change of tau in PHF-tau, also labeled CA3 neurons (Fig. 1, E–G). In summary, these findings indicate that heterozygous mPS1 mice, whose alleles most precisely reflect the genotype of humans bearing this mutation, exhibited phospho-tau accumulation with PHF-tau epitopes, whereas wPS1 mice of the same age showed no sign of tau accumulation.

Data related to the other histological criteria for NFTs confirmed these findings. In heterozygous mPS1 mice, we observed Congo red birefringence (Fig. 1, H–J) and Thioflavin T reactivity (Fig. 1K) in hippocampal neurons. The Gallyas silver staining method revealed argyrophillic neurons in the hippocampus of mPS1 mice (Fig. 1L). Argyrophillic and Congo red-positive neurons were less numerous than phospho-tau-positive neurons (less than 5% of phospho-tau-positive neurons). The tau-accumulating neurons of these mice also exhibited reduced α -tubulin immunoreactivity (Fig. 1, M and N) similar to that displayed by NFT-bearing neurons. As we previously showed in tau Tg mice (24, 25), weaker α -tubulin immunoreactivity might indicate destruction of microtubules in tau-accumulating neurons in the mPS1 mice. TUNEL staining, however, revealed no signs of apoptosis in these neurons (Fig. 1, O–R). Taken together, these results suggest that mPS1 affects the cytoskeleton of hippocampal neurons and induces NFT-like accumulation of hyperphosphorylated tau.

Biochemical and Ultrastructural Analysis of Tau in Mutant PS1 Mice—We confirmed the accumulation of NFT-like tau in mPS1 mice with biochemical and electron microscopy analyses. Because tau becomes detergent insoluble when aggregated, we assessed the amount of tau in the SDS-insoluble fraction derived from the brains of mPS1 mice. As shown in Fig. 2A, small amounts of tau were recovered in the SDS-insoluble fraction from 2-month-old mPS1 mice. The amount of tau recovered in the SDS-insoluble fraction increased with aging, and a large amount of tau was recovered from 14-month-old heterozygous mPS1 mice compared with age-matched wPS1 mice. (The amount of SDS-insoluble tau in mPS1 mice was \sim 2% of the total tau in these mice).

We also investigated the amount of SDS-insoluble tau in different brain regions of mPS1 mice. Tau was recovered from the hippocampus, and small amounts were recovered from the cerebral cortex, striatum, and cerebellum. This might be explained by the inverse correlation of NFT with pin1 expression (26).

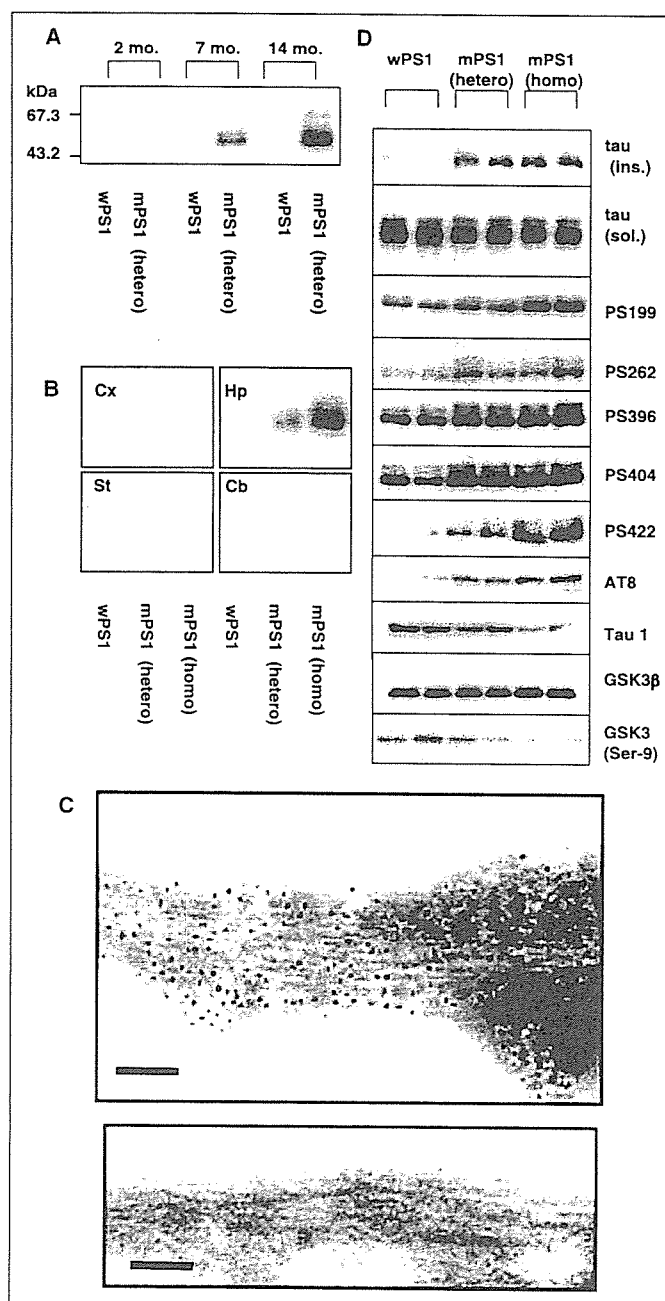


FIGURE 2. Biochemical and electron microscopy (EM) analyses of mPS1 mice. A, SDS-insoluble tau from the brains of 2-, 7-, and 14-month-old heterozygous mPS1 mice. B, SDS-insoluble tau in micro-dissected cortex (Cx), hippocampus (Hp), brainstem (St), and cerebellum (Cb) of 12-month-old wild-type PS1, heterozygous mPS1, and homozygous mPS1 mice. C, immuno-EM analysis of SDS-insoluble materials from 12-month-old heterozygous mPS1 mice. Fibrils labeled with 5-nm gold particles indicate immunoreactivity to the phosphorylation-independent tau antibody, JM (upper panel). Immunogold labeling was not observed on fibrils (control) stained in the absence of primary antibody (lower panel). Scale bars: 100 nm. D, Western blots containing SDS-insoluble and RIPA-soluble materials from the hippocampi of 14-month-old wPS1, heterozygous mPS1, and homozygous mPS1 mice. (Lane pairs correspond to a set of two mice per mouse strain.) Order of blots (from top to bottom): SDS-insoluble tau (*tau* (ins.)); RIPA-soluble tau (*tau* (sol.)); RIPA-soluble phosphorylated tau (PS199, PS262, PS396, PS404, PS422, and AT8); unphosphorylated tau (*Tau*1), active GSK3 β (GSK3 β); and inactive GSK3 β (GSK3 β Ser-9).

The SDS-insoluble material recovered from mPS1 mice were further investigated with electron microscopy. As shown in Fig. 2C, tau-positive fibrils were detected in the SDS-insoluble fraction. These fibrils appeared to be straight tubules, about 10 nm in diameter. The biochem-

Tau Inclusions in FAD Mutant PS1 Knock-in Mice

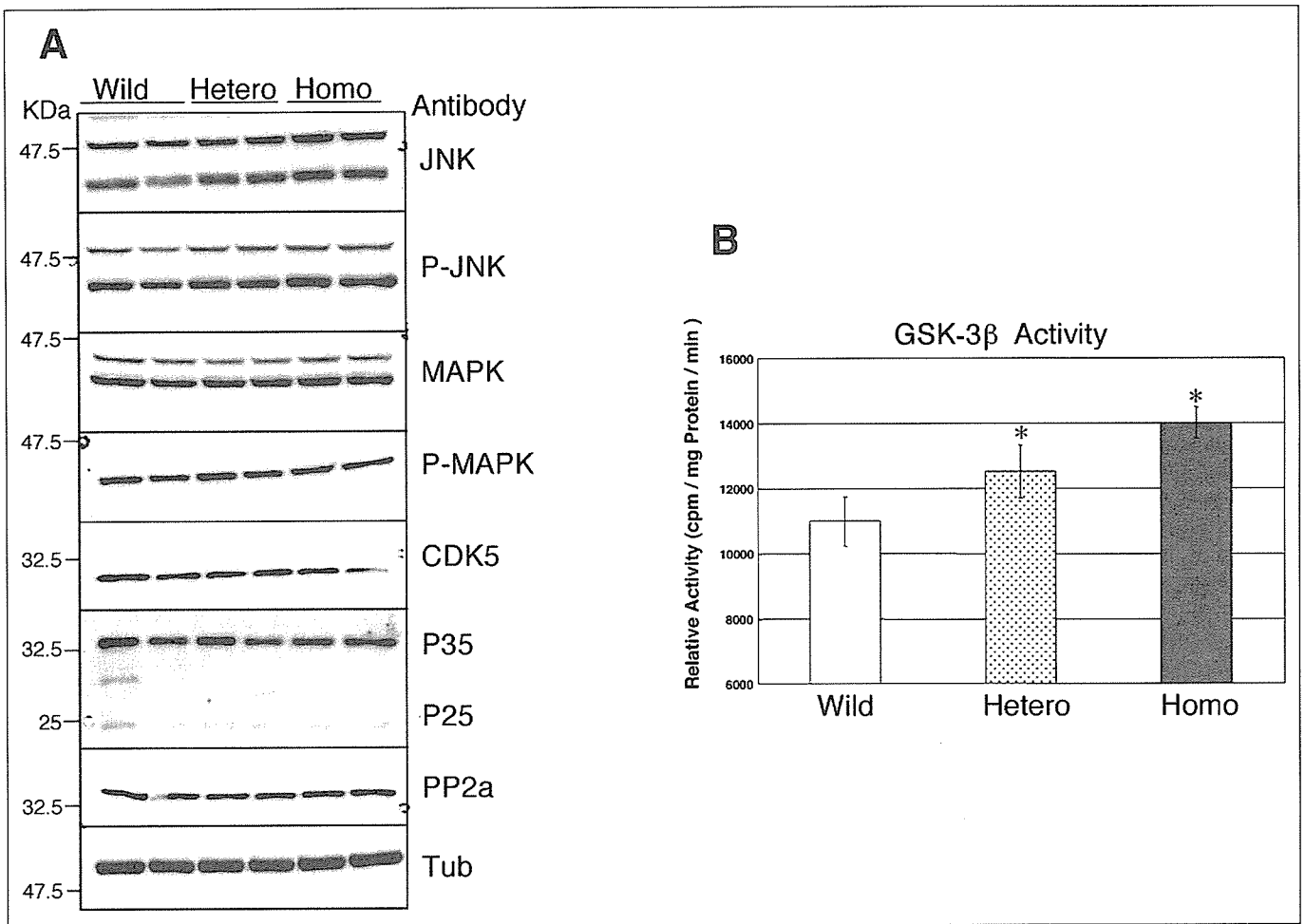


FIGURE 3. Tau kinase activity in 12-month-old mPS1 mice. *A*, hippocampal lysates from wPS1, heterozygous mPS1, and homozygous mPS1 mice were analyzed with Western blotting and antibodies against tau kinases and phosphatases: total JNK (*JNK*); phospho-JNK (*P-JNK*); MAP kinase (*MAPK*); phosphorylated MAP kinase (*PMAPK*); CDK5; the CDK5 activators, p35 and p25; and phosphatase 2a (*PP2a*). A blot stained with anti-tubulin antibody (*Tub*) represents the control. *B*, GSK-3 β activity in immunoprecipitated brain samples derived from wPS1, heterozygous mPS1, and homozygous mPS1 mice were determined with an assay that measures the incorporation of ^{32}P into a GSK-3 β substrate peptide. Data are expressed as averages \pm S.D. (*, $p < 0.05$; $n = 3$).

ical and ultrastructural analyses strongly suggest that NFT-like tau aggregation formed primarily in hippocampal neurons of mPS1 mice.

The NFTs found in AD brains contain highly phosphorylated tau (27). Hyperphosphorylation of tau leads to the formation of fibrillar tau (28). To determine whether tau hyperphosphorylation also occurs in mPS1 mice, we examined the extent of tau phosphorylation in 14-month-old wPS1, heterozygous mPS1, and homozygous mPS1 mice (Fig. 2*D*). Immunoblotting with various phosphorylation-dependent anti-tau antibodies revealed that the amount of SDS-insoluble tau was nearly the same in heterozygous and homozygous mPS1 mice (Fig. 2*D*, *tau(ins.)*). This amount, however, was greater than that in wPS1 mice. Although the total amounts of tau in soluble fractions from the three types of mice were similar (*i.e.* bands had slower mobility than the unphosphorylated Tau-1-immunoreactive band) (Fig. 2*D*, *tau(sol.)*), the amounts of phosphorylated tau immunostained by PS199, PS262, PS396, PS404, PS422, and AT8 were elevated in the heterozygous and homozygous mPS1 mice compared with those in the wPS1 mice. The extent of tau phosphorylation at the AT8, PS422, and PS199 epitopes appeared to depend on the number of mPS1 alleles present in the mice, as shown by the comparatively greater immunosignal intensity of samples derived from homozygous than in heterozygous mPS1 mice, suggesting that mPS1 expression affects the hyperphosphorylation of tau. The immunostaining intensity of Tau-1, an antibody that recognizes

unphosphorylated tau, also correlated with genotype. Tau-1 immunoreactivity was greater in samples derived from wPS1 mice than in heterozygous and homozygous mPS1 mice (wPS1 > heterozygous mPS1 > homozygous mPS1), confirming that mPS1 induced the hyperphosphorylation of tau.

GSK-3 β , Tau Kinase, and Tau Phosphatase Activity—Activation of GSK-3 β , a known tau kinase, was also associated with mPS1 genotype. Although total GSK-3 β levels were similar among wPS1, heterozygous mPS1, and homozygous mPS1 mice, inactive GSK-3 β (GSK-3 β phosphorylated at Ser-9) levels varied inversely with the number of mPS1 alleles present (Fig. 2*D*; GSK3 β and GSK3 β (Ser-9)). This inverse correlation was confirmed by comparing the GSK-3 β activity in immunoprecipitated brain samples derived from wPS1, heterozygous mPS1, and homozygous mPS1 mice (Fig. 3*B*). This assay revealed elevated GSK-3 β activity in heterozygous mPS1 compared with wPS1 mice ($p < 0.05$; $n = 3$), and also in homozygous mPS1 mice compared with heterozygous mice ($p < 0.05$; $n = 3$). Taken together, we conclude that the mutant PS1 activated GSK-3 β , thereby enhancing tau phosphorylation and resulting in the formation of NFT-like tau aggregates (Figs. 1 and 2). These results support those from a previous report (20).

We also investigated how other kinases and phosphatases may contribute to tau phosphorylation in mPS1 mice. As shown in Fig. 3*A*, levels of the active forms of phosphorylated JNK; phosphorylated MAP kinase; CDK5;

the CDK5 activators p35 and p25; and PP2a were similar among wPS1, heterozygous mPS1, and homozygous mPS1 mice, indicating that the tau phosphorylation mediated by these enzymes are not affected by the PS1 mutation. Nonetheless, other mechanisms are expected to be involved in the mPS1-induced hyperphosphorylation of tau, because GSK-3 β alone cannot phosphorylate all of the phosphorylation sites in tau.

DISCUSSION

In the present study, we demonstrated that the brains of mice harboring a PS1 mutation accumulated NFT-like phospho-tau. Biochemical analysis of SDS-insoluble tau revealed tau fibrils. These NFT-like tau inclusions were similar to those observed in FTDP-17 mutant tau transgenic mice (24, 25, 28), in mice overexpressing p25, a CDK5 activator (29), and in Pin1 knock-out mice (26). The neurons of other PS1 knock-in and mutant PS1 transgenic mice; however, failed to show cytoskeletal changes (30, 31). To create their mutant PS1 knock-in mice, Guo *et al.* (32) used a hybrid mouse composed of 129SV and C57BL6 strains, whereas in the present study we used mice resulting from 10 generations of crossbreeding with C57BL6J mice. The genetic background of our mice, which is most likely to be different from the backgrounds of mice used in previously studies, could have influenced how the PS1 mutation contributed to NFT formation and cytoskeletal changes. Another possible explanation for the apparent discrepancy between our findings and others is that our PS1 knock-in mice harbored a different PS1 mutation from that harbored by mutant PS1 knock-in mice developed by other laboratories.

Previously, we found certain PS1 mutations that increase A β ₁₋₄₂ levels are poor predictors for the onset of FAD (5). Our present results, however, suggest that the accumulation of NFT-like tau could determine the onset of AD. These two differing outcomes would also explain why some PS1 mutations accelerate NFT formation and neuronal loss without accelerating A β deposition (18). Thus, PS1 mutations that accelerate both NFT formation and A β ₁₋₄₂ production may further accelerate related neuropathologies, suggesting that the cause of early onset AD may be related to a PS1 mutation.

The mechanism underlying the mutant PS1-associated accumulation of NFTs may involve the activation of GSK-3 β . Our results indicate that GSK-3 β is activated in our mPS1 knock-in mice; this is consistent with other mPS1 transgenic mice. Recently, wild-type PS1 has been shown to activate PI3 kinase/Akt signaling by promoting the association of cadherin and PI 3-kinase, whereas mutant PS1 was unable to do so (32). Thus, mutant PS1 appears to impair PI 3-kinase/Akt signaling by affecting selected signaling receptors (33) or by reducing cadherin/PI3 kinase association (32), which eventually leads to the activation of GSK-3 β . Whereas the mutant PS1-associated activation of GSK-3 β occurred in young mice, tau accumulation occurred only later on in older mice. This led us to hypothesize that, by some mechanism, phosphorylated tau degrades before it aggregates. This unknown mechanism is then inactivated during aging, leading to the accumulation and aggregation of tau that occurs in aged individuals.

Patients harboring the FAD mutation of PS1 develop AD with 100% penetration. Based on our results, we propose that the PS1 mutation in FAD leads to the early onset of AD through the activation of GSK-3 β , which leads to NFT formation and the loss of neurons and synapses. Moreover, we believe that the rate of GSK-3 β activation is accelerated by extracellular A β oligomers. The exact molecular mechanism mediating the mutant PS1-induced activation of GSK-3 β requires clarification to further our understanding of how AD develops.

REFERENCES

1. Sherrington, R., Rogaev, E. I., Liang, Y., Rogaeva, E. A., Levesque, G., Ikeda, M., Chi, H., Lin, C., Li, G., Holman, K., Tsuda, T., Mar, L., Foncin, J.-F., Bruni, A. C., Montesi,

- M. P., Sorbi, S., Rainero, I., Pinessi, L., Nee, L., Chumakov, I., Pollen, D., Brookes, A., Sanseau, P., Polinsky, R. J., Wasco, W., Da Silva, H. A. R., Haines, J. L., Pericak-Vance, M. A., Tanzi, R. E., Roses, A. D., Fraser, P. E., Rommens, J. M., and St. George-Hyslop, P. H. (1995) *Nature* **375**, 754–760
2. Cruts, M., Backhovens, H., Wang, S. Y., Van Gassen, G., Theuns, J., De Jonghe, C. D., Wehnert, A., De Voecht, J., De Winter, G., and Cras, P. (1995) *Hum. Mol. Genet.* **4**, 2363–2371
3. St George-Hyslop, P. H., and Petit, A. (2005) *C. R. Biol.* **328**, 119–130
4. St George-Hyslop, P. H. (2000) *Biol. Psychiatry* **47**, 183–199
5. Murayama, O., Honda, T., Mercken, M., Murayama, M., Yasutake, K., Nihonmatsu, N., Nakazato, Y., Michel, G., Song, S., Sato, K., Takahashi, H., and Takashima, A. (1997) *Neurosci. Lett.* **229**, 61–64
6. Scheuner, D., Eckman, C., Jensen, M., Song, X., Citron, M., Suzuki, N., Bird, T. D., Hardy, J., Hutton, M., Kukull, W., Larson, E., Levy-Lahad, E., Viitanen, M., Peskind, E., Poorkaj, P., Schellenberg, G., Tanzi, R., Wasco, W., Lannfelt, L., Selkoe, D., and Younkin, S. (1996) *Nat. Med.* **2**, 864–870
7. Holcomb, L., Gordon, M. N., McGowan, E., Yu, X., Benkovic, S., Jantzen, P., Wright, K., Saad, I., Mueller, R., Morgan, D., Sanders, S., Zehr, C., O'Campo, K., Hardy, J., Prada, C. M., Eckman, C., Younkin, S., Hsiao, K., and Duff, K. (1998) *Nat. Med.* **4**, 97–100
8. Chang, P., and Su, Y. (2000) *Brain Res. Brain Res. Protoc.* **6**, 6–12
9. Klein, A. M., Kowall, N. W., and Ferrante, R. J. (1999) *Ann. N. Y. Acad. Sci.* **893**, 314–320
10. Morelli, L., Prat, M. I., and Castano, E. M. (1999) *Cell Tissue Res.* **298**, 225–232
11. Butterfield, D. A. (2002) *Free Radic. Res.* **36**, 1307–1313
12. Yu, H., Saura, C. A., Choi, S. Y., Sun, L. D., Yang, X., Handler, M., Kawarabayashi, T., Younkin, L., Fedele, B., Wilson, M. A., Younkin, S., Kandel, E. R., Kirkwood, A., and Shen, J. (2001) *Neuron* **31**, 713–726
13. Amtul, Z., Lewis, P. A., Piper, S., Crook, R., Baker, M., Findlay, K., Singleton, A., Hogg, M., Younkin, L., Younkin, S. G., Hardy, J., Hutton, M., Boeve, B. F., Tang-Wai, D., and Golde, T. E. (2002) *Neurobiol. Dis.* **9**, 269–273
14. Dermaut, B., Kumar-Singh, S., Engelborghs, S., Theuns, J., Rademakers, R., Saerens, J., Pickut, B. A., Peeters, K., van den Broeck, M., Vennekens, K., Claes, S., Cruts, M., Cras, P., Martin, J. J., Van Broeckhoven, C., and De Deyn, P. P. (2004) *Ann. Neurol.* **55**, 617–626
15. Tang-Wai, D., Lewis, P., Boeve, B., Hutton, M., Golde, T., Baker, M., Hardy, J., Michels, V., Ivnik, R., Jack, C., and Petersen, R. (2002) *Dement. Geriatr. Cogn. Disord.* **14**, 13–21
16. Evin, G., Smith, M. J., Tziotis, A., McLean, C., Canterford, L., Sharples, R. A., Cappai, R., Weidemann, A., Beyreuther, K., Cotton, R. G., Masters, C. L., and Culvenor, J. G. (2002) *Neuroreport* **13**, 719–723
17. Yoshiyama, Y., Lee, V. M., and Trojanowski, J. Q. (2001) *Curr. Neurol. Neurosci. Rep.* **1**, 413–421
18. Gomez-Isla, T., Growdon, W. B., McNamara, M. J., Nochlin, D., Bird, T. D., Arango, J. C., Lopera, F., Kosik, K. S., Lantos, P. L., Cairns, N. J., and Hyman, B. T. (1999) *Brain* **122**, 1709–1719
19. Nakano, Y., Kondoh, G., Kudo, T., Imaizumi, K., Kato, M., Miyazaki, J. I., Tohyama, M., Takeda, J., and Takeda, M. (1999) *Eur. J. Neurosci.* **11**, 2577–2581
20. Takashima, A., Murayama, M., Murayama, O., Kohno, T., Honda, T., Yasutake, K., Nihonmatsu, N., Mercken, M., Yamaguchi, H., Sugihara, S., and Wolozin, B. (1998) *Proc. Natl. Acad. Sci. U. S. A.* **95**, 9637–9641
21. Van Lint, J., Khandelwal, R. L., Merlevede, W., and Vandenheede, J. R. (1993) *Anal. Biochem.* **208**, 132–137
22. Iqbal, K., Braak, E., Braak, H., Zaidi, T., and Grundke-Iqbal, I. (1991) *Neurobiol. Aging* **12**, 357–361
23. Sun, X., Cole, G. M., Chu, T., Xia, W., Galasko, D., Yamaguchi, H., Tanemura, K., Frautschy, S. A., and Takashima, A. (2002) *Neurobiol. Aging* **23**, 195–203
24. Tatebayashi, Y., Miyasaka, T., Chui, D. H., Akagi, T., Mishima, K., Iwasaki, K., Fujiwara, M., Tanemura, K., Murayama, M., Ishiguro, K., Planel, E., Sato, S., Hashikawa, T., and Takashima, A. (2002) *Proc. Natl. Acad. Sci. U. S. A.* **99**, 13896–13901
25. Tanemura, K., Murayama, M., Akagi, T., Hashikawa, T., Tominaga, T., Ichikawa, M., Yamaguchi, H., and Takashima, A. (2002) *J. Neurosci.* **22**, 133–141
26. Liou, Y. C., Sun, A., Ryo, A., Zhou, X. Z., Yu, Z. X., Huang, H. K., Uchida, T., Bronson, R., Bing, G., Li, X., Hunter, T., and Lu, K. P. (2003) *Nature* **424**, 556–561
27. Lee, V. M., Balin, B. J., Otvos, L., Jr., and Trojanowski, J. Q. (1991) *Science* **251**, 675–678
28. Sato, S., Tatebayashi, Y., Akagi, T., Chui, D. H., Murayama, M., Miyasaka, T., Planel, E., Tanemura, K., Sun, X., Hashikawa, T., Yoshioka, K., Ishiguro, K., and Takashima, A. (2002) *J. Biol. Chem.* **277**, 42060–42065
29. Cruz, J. C., Tseng, H. C., Goldman, J. A., Shih, H., and Tsai, L. H. (2003) *Neuron* **40**, 471–483
30. Siman, R., Reaume, A. G., Savage, M. J., Trusko, S., Lin, Y. G., Scott, R. W., and Flood, D. G. (2000) *J. Neurosci.* **20**, 8717–8726
31. Guo, Q., Sebastian, L., Sopher, B. L., Miller, M. W., Ware, C. B., Martin, G. M., and Mattson, M. P. (1999) *J. Neurochem.* **72**, 1019–1029
32. Baki, L., Shioi, J., Wen, P., Shao, Z., Schwarzman, A., Gama-Sosa, M., Neve, R., and Robakis, N. K. (2004) *EMBO J.* **23**, 2586–2596
33. Kang, D. E., Sang Yoon, I., Repetto, E., Busse, T., Yermian, N., Ie, L., and Koo, E. H. (2005) *J. Biol. Chem.* **280**, 31537–31547